

The CF₃CH₂O[−] Adducts of α-Nitro-β-(2,2,2-trifluoroethoxy)stilbene and β-Methoxy-α-nitrostilbene, and the MeO[−] Adduct of β-Methoxy-α-nitrostilbene. Kinetics of Competition between Protonation and Acid Catalyzed Alkoxide Ion Departure

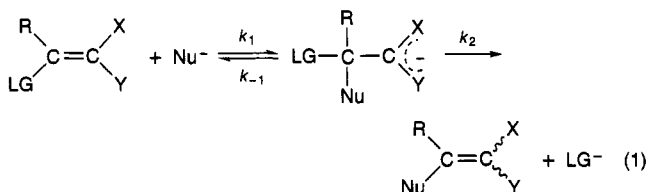
Claude F. Bernasconi,^{*,†} David F. Schuck,[†] Rodney J. Ketner,[†]
Irina Eventova,[‡] and Zvi Rappoport[‡]

Contribution from the Department of Chemistry and Biochemistry, University of California, Santa Cruz, California 95064, and the Department of Organic Chemistry, The Hebrew University, Jerusalem 91904, Israel

Received September 29, 1994[®]

Abstract: The reaction of aqueous acids with the CF₃CH₂O[−] adduct, Ph(OCH₂CF₃)₂CC(Ph)=NO₂[−], of α-nitro-β-(2,2,2-trifluoroethoxy)stilbene leads virtually exclusively to the corresponding acetal, Ph(OCH₂CF₃)₂CCH(Ph)NO₂, by carbon protonation, whereas reaction of acid with the CH₃O[−] adduct, Ph(OCH₃)₂CC(Ph)=NO₂[−], of β-methoxy-α-nitrostilbene leads virtually exclusively to recovery of the β-methoxy-α-nitrostilbene by acid catalyzed CH₃O[−] expulsion. In the case of Ph(OCH₃)(OCH₂CF₃)CC(Ph)=NO₂[−], reaction with HCl produces a mixture of the corresponding acetal, Ph(OCH₃, OCH₂CF₃)CCH(Ph)NO₂, β-methoxy-α-nitrostilbene and α-nitro-β-(2,2,2-trifluoroethoxy)stilbene. Rate constants for these processes as well as for the deprotonation of the various acetals by OH[−] and amines are reported. The large difference in the kinetic behavior of the various adducts as a function of the alkoxy groups is attributed to a combination of factors. They include the strong dependence of acid catalysis on leaving group basicity, the much stronger push by the methoxy compared to the trifluoroethoxy group, and the manifestation of the nitroalkane anomaly according to which a more basic nitronate ion is protonated more slowly than a less basic one.

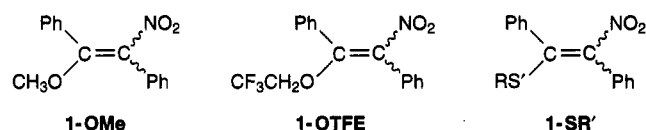
In our attempt at better understanding the structure–reactivity relationships that govern the addition–elimination mechanism of nucleophilic vinylic substitution (S_NV) reactions,¹ we have been searching for systems in which the tetrahedral intermediate is detectable. Such systems allow a kinetic determination of the rate not only of the nucleophilic attack step (*k*₁) but also of *k*_{−1} and *k*₂, which provide information about the nucleofugality



of the leaving group and the nucleophile. In view of the scarce data on nucleofugalities in S_NV reactions,² such information is particularly valuable.

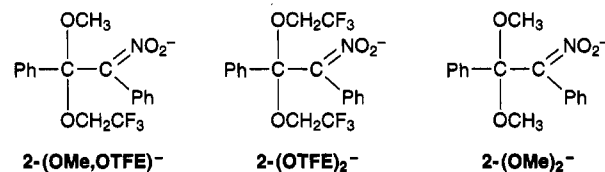
Systems investigated to date that have yielded a detectable intermediate include the reactions of **1-OMe** with CH₃O[−],³

CF₃CH₂O[−],⁴ MeONHCH₃,⁵ and various alkanethiolate ions (RS[−]),⁶ of **1-OTFE** with CF₃CH₂O[−],⁴ HOCH₂CH₂S[−], and



piperidine⁴ and of **1-SR'** (R' = CH₃CH₂CH₂, HOCH₂CH₂, and CH₃O₂CCH₂CH₂) with various RS[−].⁶

In studying the intermediates generated by CF₃CH₂O[−] addition to **1-OMe**, **2-(OMe,OTFE)**[−],⁴ by CF₃CH₂O[−] addition to **1-OTFE**, **2-(OTFE)₂**[−],⁴ and by CH₃O[−] addition to **1-OMe**,



2-(OMe)₂,^{−3} we made the following observations.

(1) In basic solution, the rate constant for CF₃CH₂O[−] loss from **2-(OTFE)₂**[−] is 1.65 × 10^{−5} s^{−1}, that for CF₃CH₂O[−] loss from **2-(OMe,OTFE)**[−] is 5.0 × 10^{−5} s^{−1}, and that for loss of

(4) Bernasconi, C. F.; Schuck, D. F.; Ketner, R. J.; Weiss, M.; Rappoport, Z. *J. Am. Chem. Soc.* **1994**, *116*, 11764.

(5) Bernasconi, C. F.; Leyes, A. E.; Rappoport, Z.; Eventova, I. *J. Am. Chem. Soc.* **1993**, *115*, 7513.

(6) (a) Bernasconi, C. F.; Killion, R. B., Jr.; Fassberg, J.; Rappoport, Z. *J. Am. Chem. Soc.* **1989**, *111*, 6862. (b) Bernasconi, C. F.; Fassberg, J.; Killion, R. B.; Rappoport, Z. *J. Am. Chem. Soc.* **1990**, *112*, 3169.

[†] University of California.

[‡] The Hebrew University.

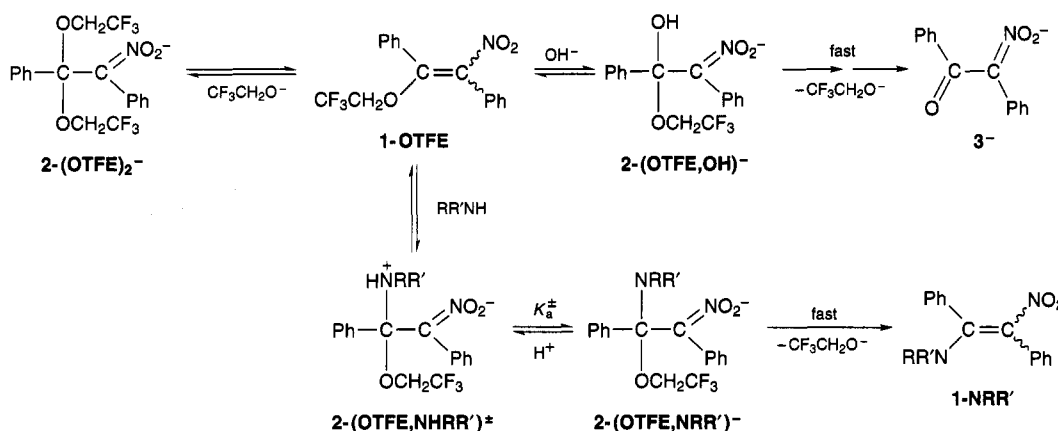
[®] Abstract published in *Advance ACS Abstracts*, February 15, 1995.

(1) For reviews, see: (a) Rappoport, Z. *Adv. Phys. Org. Chem.* **1969**, *7*, 1. (b) Modena, G. *Acc. Chem. Res.* **1971**, *4*, 73. (c) Miller, S. I. *Tetrahedron* **1977**, *33*, 1211. (d) Rappoport, Z. *Acc. Chem. Res.* **1981**, *14*, 7. (e) Rappoport, Z. *Recl. Trav. Chim. Pays-Bas* **1985**, *104*, 309. (f) Shainyan, B. A. *Usp. Khim.* **1986**, *55*, 942. (g) Rappoport, Z. *Acc. Chem. Res.* **1992**, *25*, 474.

(2) Bernasconi, C. F. *Tetrahedron* **1989**, *45*, 4017.

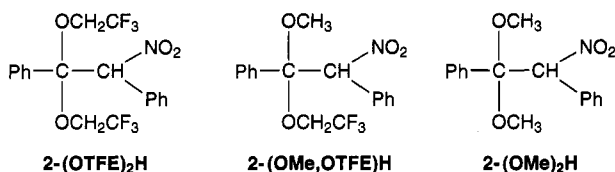
(3) Bernasconi, C. F.; Fassberg, J.; Killion, R. B.; Schuck, D. F.; Rappoport, Z. *J. Am. Chem. Soc.* **1991**, *113*, 4937.

Scheme 1



CH_3O^- from 2-(OMe)_2^- is $4.0 \times 10^{-8} \text{ s}^{-1}$, whereas the loss of CH_3O^- from 2-(OMe,OTFE)^- was too slow to measure ($< 4 \times 10^{-8} \text{ s}^{-1}$). These results indicate that, among other things, departure of oxyanion leaving groups from $\text{S}_\text{N}\text{V}$ intermediates is highly sensitive to leaving group basicity, with $\beta_{1\beta}$ values close to -1.

(2) In acidic solution, 2-(OTFE)_2^- is virtually quantitatively converted to $2\text{-(OTFE)}_2\text{H}$ by protonation. This contrasts with



2-(OMe)_2^- which does not form $2\text{-(OMe)}_2\text{H}$ but yields **1-OMe** by acid catalyzed loss of methoxide ion, while 2-(OMe,OTFE)^- shows intermediate behavior in that protonation competes with acid catalyzed methoxide as well as $\text{CF}_3\text{CH}_2\text{O}^-$ departure to yield a mixture of 2-(OMe,OTFE)H , **1-OMe**, and **1-OTFE**. Incidentally, the reaction of 2-(OMe,OTFE)^- with acid is thus far the only known method to generate **1-OTFE** in isolable quantities.⁴

In the present paper we report a kinetic study of the reactions of 2-(OTFE)_2^- and 2-(OMe,OTFE)^- with acid, to be compared with a previous kinetic investigation of 2-(OMe)_2^- ,³ as well as of the deprotonation of $2\text{-(OTFE)}_2\text{H}$, 2-(OMe,OTFE)H , and $2\text{-(OMe)}_2\text{H}$, by a variety of bases. Our main objective is to develop a better understanding of why 2-(OTFE)_2^- , 2-(OMe,OTFE)^- , and 2-(OMe)_2^- behave so differently from each other in acidic solution.

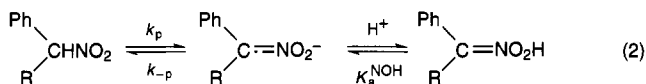
Results

General Features. All kinetic experiments were performed in 50% Me_2SO –50% water (v/v) at 20 °C. The ionic strength was maintained at 0.5 M with KCl. Pseudo-first-order conditions with the substrates as the minor component were used throughout.

Kinetics of Deprotonation of $2\text{-(OTFE)}_2\text{H}$ /Protonation of 2-(OTFE)_2^- . $2\text{-(OTFE)}_2\text{H}$ is a phenylnitromethane derivative whose kinetic behavior is quite similar to that of phenylnitromethane. Hence the methodology used in studying the proton transfer kinetics was essentially the same as that described earlier for PhCH_2NO_2 ⁷ and is only briefly summarized here.

The reaction scheme is shown in eq 2 with $\text{R} = \text{PhC}(\text{OCH}_2\text{CF}_3)_2$, and k_p and k_{-p} are given by eqs 3 and 4. The pseudo-first-order rate constant for equilibrium approach is given by

eq 5. Note that the $K_a^{\text{NOH}}/(K_a^{\text{NOH}} + a_{\text{H}^+})$ term is unity under



$$k_p = k_p^{\text{H}_2\text{O}} + k_p^{\text{OH}} a_{\text{OH}^-} + k_p^{\text{B}} [\text{B}] \quad (3)$$

$$k_{-p} = k_{-p}^{\text{H}^+} a_{\text{H}^+} + k_{-p}^{\text{H}_2\text{O}} + k_{-p}^{\text{BH}} [\text{BH}] \quad (4)$$

$$k_{\text{obsd}} = k_p + k_{-p} \frac{K_a^{\text{NOH}}}{K_a^{\text{NOH}} + a_{\text{H}^+}} \quad (5)$$

most conditions except at low pH where a_{H^+} becomes comparable to K_a^{NOH} or exceeds it.

The kinetics was followed in a stopped-flow or conventional spectrophotometer by approaching the equilibrium either from the nitroalkane side ($\text{pH} > \text{p}K_a^{\text{CH}}$ with $\text{p}K_a^{\text{CH}}$ referring to the $\text{p}K_a$ of the carbon acid) or from the nitronate side ($\text{pH} < \text{p}K_a^{\text{CH}}$). For the latter “pH-jump” experiments, the nitronate ion was first generated in a 0.01 M KOH solution, a process that takes $< 1 \text{ s}$. This solution was then mixed with the appropriate acidic buffer. Since the nitronate ion gradually decomposes into 3^- (Scheme 1), these experiments were performed shortly after the nitronate ion had been generated.

In KOH solution, with $\text{CF}_3\text{CH}_2\text{O}^-$ and with the amine bases, all experiments were performed in the direction $\text{Ph(R)CHNO}_2 \rightarrow \text{Ph(R)C=NO}_2^-$. The kinetic traces were biphasic, with the fast phase referring to the proton transfer and the slow phase to the formation of 3^- (in $\text{CF}_3\text{CH}_2\text{O}^-$ buffers and KOH solution) or of **1-NRR'** in amine buffers (Scheme 1). These latter products are formed by reaction of OH^- or the amine with **1-OTFE** generated by loss of $\text{CF}_3\text{CH}_2\text{O}^-$ from 2-(OTFE)_2^- (Scheme 1) as described previously.⁴ The slow phase was slow enough as not to seriously interfere with the determination of k_{obsd} of the fast phase, although corrections for a sloping “infinity” line were necessary.

Individual second-order rate constants were obtained from k_{obsd} measured at 5 to 7 different [KOH] or buffer concentrations; these data are summarized in Tables S1–S3 of the supplementary material.⁸ All plots of k_{obsd} vs buffer concentration (not shown) were linear; the second-order rate constants calculated from the slopes of the buffer plots are summarized in Table 1. In evaluating the second-order rate constants for the reaction with $\text{CF}_3\text{CH}_2\text{O}^-$, association of $\text{CF}_3\text{CH}_2\text{O}^-$ with $\text{CF}_3\text{CH}_2\text{OH}$ ($K_{\text{assoc}} \approx 2 \text{ M}^{-1}$)⁴ was taken into account in calculating the concentration of free $\text{CF}_3\text{CH}_2\text{O}^-$ (Table S3).⁸

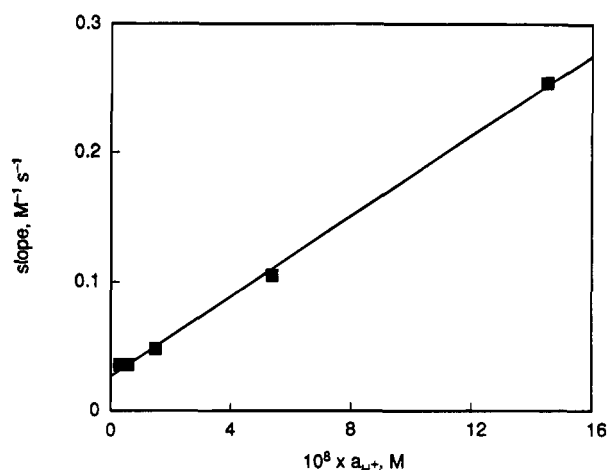
The determination of $\text{p}K_a^{\text{CH}}$ by classical spectrophotometric methodology was rendered difficult because of the decom-

(7) Bernasconi, C. F.; Kliner, D. A. V.; Mullin, A. S.; Ni, J. X. *J. Org. Chem.* **1988**, *53*, 3342.

Table 1. Rate Constants ($M^{-1} s^{-1}$) and pK_a Values for the Reversible Deprotonation of 2-(OTFE)₂H, 2-(OMe,OTFE)H, and 2-(OMe)₂H in 50% Me₂SO–50% Water at 20 °C^{a,b}

B	pK_a^{BH}	2-(OTFE) ₂ H ($pK_a^{CH} = 7.79$)		2-(OMe,OTFE)H ($pK_a^{CH} = 8.51$)		2-(OMe) ₂ H ($pK_a^{CH} = 8.89$)	
		k_p^B	k_{-p}^{BH}	k_p^B	k_{-p}^{BH}	k_p^B	k_{-p}^{BH}
OH ⁻	17.34	1.15×10^3	$9.01 \times 10^{-6}^c$	1.55×10^2	$6.32 \times 10^{-6}^c$	25.0	$2.50 \times 10^{-6}^c$
CF ₃ CH ₂ O ⁻	14.0	6.86×10^2	4.22×10^{-4}				
piperidine	11.02	1.61	9.47×10^{-4}	2.73×10^{-1}	8.45×10^{-4}	6.87×10^{-2}	5.10×10^{-4}
morpholine	8.72	7.25×10^{-2}	8.52×10^{-3}	1.28×10^{-2}	7.88×10^{-3}	4.48×10^{-3}	6.63×10^{-3}
<i>n</i> -BuNH ₂	10.65	1.29	1.78×10^{-3}	2.02×10^{-1}	1.47×10^{-3}	4.64×10^{-2}	8.06×10^{-4}
CH ₃ OCH ₂ CH ₂ NH ₂	9.46	2.57×10^{-1}	3.81×10^{-3}	2.83×10^{-2}	3.18×10^{-3}	1.22×10^{-2}	2.27×10^{-3}
H ₂ NCOCH ₂ NH ₂	8.27	2.24×10^{-2}	7.41×10^{-3}	4.93×10^{-3}	8.58×10^{-3}	1.67×10^{-3}	6.94×10^{-3}
EtOOCCH ₂ NH ₂	7.87	2.50×10^{-2}	2.10×10^{-2}	3.54×10^{-3}	1.55×10^{-2}	1.13×10^{-3}	1.18×10^{-3}
CH ₃ OCH ₂ COOH	4.56	4.84×10^{-4}	8.16×10^{-1}	4.04×10^{-5}	3.60×10^{-1}		
H ₂ O	-1.44	$5.09 \times 10^{-7}^c$	30.8	$6.24 \times 10^{-8}^c$	20.2		

^a $\mu = 0.5$ M (KCl). ^b The standard deviations of most k_p^B and k_{-p}^{BH} values are less than 5%. In the reactions of 2-(OMe,OTFE)H with OH⁻, CF₃CH₂O⁻, and amines the actual error in the k_p^B and k_{-p}^{BH} values is estimated at $\pm 10\%$ for reasons explained in the text. ^c Units of s⁻¹.

**Figure 1.** Reaction of 2-(OTFE)₂H with EtOOCCH₂NH₂. Plot of slopes vs a_{H^+} according to eq 6.

position of R(Ph)C=NO₂⁻ into 3⁻ mentioned above. Hence pK_a^{CH} was obtained kinetically from rate measurements in glycine ethyl ester buffers. The slope of a plot of k_{obsd} vs glycine ethyl ester concentration ($[B]$) is given by eq 6 with K_a^{BH} being the acid dissociation constant of BH. Figure 1 shows a plot of

$$\text{slope} = k_p^B + k_{-p}^{BH} \frac{a_{H^+}}{K_a^{BH}} \quad (6)$$

slope vs a_{H^+} with slopes determined at pH 6.84, 7.27, 7.83, 8.25, and 8.54 (Table S5).⁸ It yields $k_p^B = (2.50 \pm 0.20) \times 10^{-2} M^{-1} s^{-1}$ and $k_{-p}^{BH} = (2.10 \pm 0.18) \times 10^{-2} M^{-1} s^{-1}$ ($pK_a^{BH} = 7.87$) from which $K_a^{CH} = K_a^{BH} k_p^B / k_{-p}^{BH} = (1.61 \pm 0.27) \times 10^{-9}$ or $pK_a^{CH} = 7.79 \pm 0.07$ is obtained.

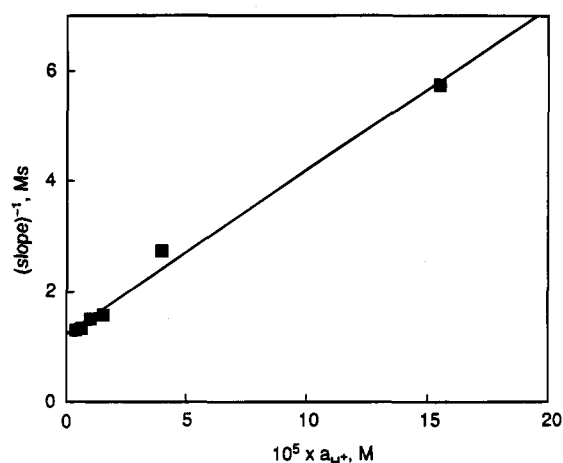
Rate measurements by pH-jump into methoxyacetic acid buffer solutions (Table S4)⁸ allowed a kinetic determination of pK_a^{NOH} . In such solutions eq 5 takes on the form of eq 7. Plots

$$k_{obsd} = (k_{-p}^H a_{H^+} + k_{-p}^{BH} [BH]) \frac{K_a^{NOH}}{K_a^{NOH} + a_{H^+}} \quad (7)$$

of k_{obsd} vs $[BH]$ afford slopes which, after inversion, are given by eq 8. Figure 2 shows a plot of $(\text{slope})^{-1}$ vs a_{H^+} (Table S6)⁸

$$\frac{1}{\text{slope}} = \frac{1}{k_{-p}^{BH}} + \frac{a_{H^+}}{K_a^{NOH} k_{-p}^{BH}} \quad (8)$$

(8) See paragraph concerning supplementary materials at the end of this paper.

**Figure 2.** Reaction of 2-(OTFE)₂⁻ with methoxyacetic acid (pH-jumps). Plot of $(\text{slope})^{-1}$ vs a_{H^+} according to eq 8.

according to eq 8 from which $pK_a^{NOH} = 4.38 \pm 0.08$ and $k_{-p}^{BH} = 0.82 \pm 0.12 M^{-1} s^{-1}$ is obtained. The reciprocal intercepts of plots of k_{obsd} vs $[BH]$ are given by eq 9. These reciprocal

$$\frac{1}{\text{intercept}} = \frac{1}{K_a^{NOH} k_{-p}^H} + \frac{1}{k_{-p}^H a_{H^+}} \quad (9)$$

intercepts are summarized in Table S6;⁸ a plot (not shown) according to eq 9 affords $k_{-p}^H = 31.6 \pm 1.3 M^{-1} s^{-1}$ and $pK_a^{NOH} = 4.34 \pm 0.10$. This latter value is in excellent agreement with the pK_a^{NOH} value obtained from eq 9; we shall adopt the average (4.36) as pK_a^{NOH} . As to k_{-p}^H , a small correction will have to be applied as described in the next section.

Product Study of the Reaction of 2-(OTFE)₂⁻ with HCl.

The analysis of the pH-jump data described in the previous section is based on the assumption that protonation of 2-(OTFE)₂⁻ is the sole reaction, i.e., acid catalyzed CF₃CH₂O⁻ departure is too slow to significantly compete with proton transfer. UV spectra of infinity solutions indicated that this is a good approximation. Nevertheless, it seemed of interest to determine whether 1-OTFE is formed in trace amounts. An HPLC analysis (see Experimental Section) showed that approximately 2.5% of 1-OTFE is recovered in pH-jump experiments with HCl. This implies that the value of $31.6 M^{-1} s^{-1}$ obtained for k_{-p}^H from our kinetic analysis actually refers to $k_{-p}^H + k_{-1}^H$, with $k_{-1}^H = 0.80 M^{-1} s^{-1}$ (2.5% of 31.6) referring to H⁺-catalyzed loss of CF₃CH₂O⁻; the corrected value for k_{-p}^H is thus $30.8 M^{-1} s^{-1}$.

Kinetics of Deprotonation of 2-(OMe)₂H. The kinetic behavior of 2-(OMe)₂H is very similar to that of 2-(OTFE)₂H.

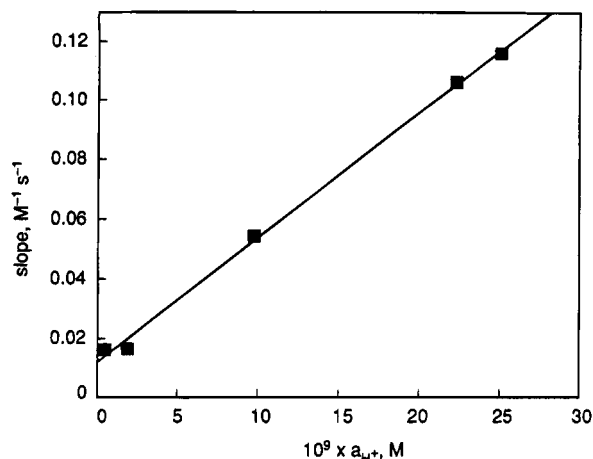


Figure 3. Reaction of 2-(OMe,OTFE)H with morpholine. Plot of slope vs a_{H^+} according to eq 6.

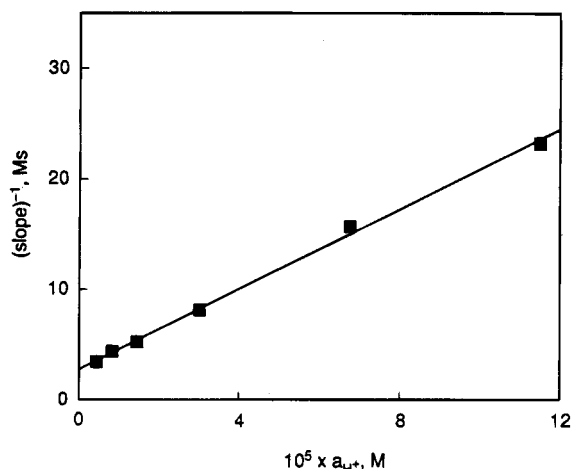


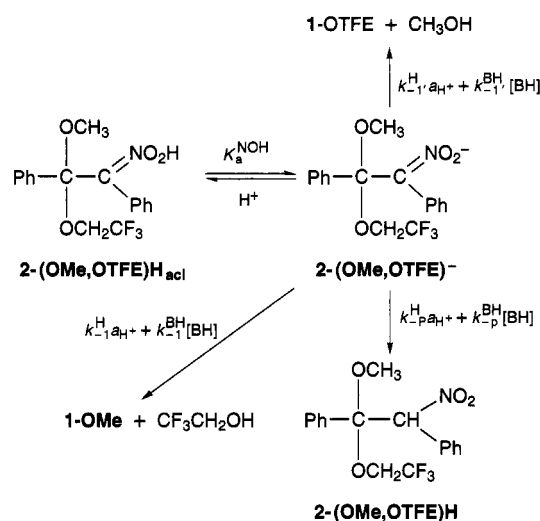
Figure 4. Reaction of 2-(OMe,OTFE)[−] with methoxyacetic acid (pH-jumps). Plot of (slope)^{−1} vs a_{H^+} according to eq 8.

One difference is that 2-(OMe)₂[−] is more stable in basic solution than 2-(OTFE)₂[−] because the loss of CH₃O[−] from 2-(OMe)₂[−] is slower than the loss of CF₃CH₂O[−] from 2-(OTFE)₂[−] (Scheme 1). This allowed a spectrophotometric determination of pK_a^{CH} (8.89 ± 0.06) (Table S7)⁸ and also eliminated the interference of the decomposition of 2-(OMe)₂[−] with the kinetic measurements of the proton transfer. Another difference is that the reaction of 2-(OMe)₂[−] with carboxylic acids or HCl does not lead to protonation but to acid catalyzed loss of CH₃O[−] to yield 1-OMe as reported before.³ All proton transfer rate constants determined with this compound are summarized in Table 1 while the raw data are in Tables S8 and S9.⁸

Kinetics of Deprotonation of 2-(OMe,OTFE)H. Of the three acetals, 2-(OMe,OTFE)H is the least stable in basic solution because CF₃CH₂O[−] loss is substantially faster from 2-(OMe,OTFE)[−] than from 2-(OTFE)₂[−]. (A scheme similar to Scheme 1 applies.) Hence the separation between the rate of proton transfer and that of the loss of CF₃CH₂O[−] was much weaker than in the deprotonation of 2-(OTFE)₂H. As a consequence, the estimated error in the proton transfer rate constants (Table 1) is somewhat higher than for the other two acetals and assumed to be twice the standard deviation. As with 2-(OTFE)₂H, the pK_a^{CH} of 2-(OMe,OTFE)H was determined kinetically according to eq 6; in this case morpholine served as the buffer. It yielded $pK_a^{CH} = 8.51$ from a plot of slopes vs a_{H^+} (Figure 3). All the raw data are summarized in Tables S10 and S11.⁸

Reaction of 2-(OMe,OTFE)[−] with Acid. A. **Kinetics.** When 2-(OMe,OTFE)[−] is subjected to a pH-jump in an HCl

Scheme 2



or a carboxylic acid buffer, one might expect a reaction pattern which lies somewhere between that observed for 2-(OTFE)₂[−] and 2-(OMe)₂[−], i.e., there may be a competition between protonation and acid catalyzed loss of one or both alkoxy groups. The various possible pathways are shown in Scheme 2.

According to Scheme 2, k_{obsd} should be given by eq 10.

$$k_{obsd} = (k_{-p}^H + k_{-1}^H + k_{-1'}^H)a_{H^+} \frac{K_a^{NOH}}{K_a^{NOH} + a_{H^+}} + (k_{-p}^{BH} + k_{-1}^{BH} + k_{-1'}^{BH})[BH] \frac{K_a^{NOH}}{K_a^{NOH} + a_{H^+}} \quad (10)$$

Experiments with HCl in the range from 0.001 to 0.1 M yielded a mixture of 1-OMe, 1-OTFE, and 2-(OMe,OTFE)H as determined by UV spectroscopy and HPLC analysis (more on this below). k_{obsd} was found to be pH independent (Table S14)⁸ and have a value of $(1.20 \pm 0.05) \times 10^{-3} \text{ s}^{-1}$. The pH independence is consistent with eq 10 which simplifies to eq 11 ($K_a^{NOH} \ll a_{H^+}$) under these conditions.

$$k_{obsd} = (k_{-p}^H + k_{-1}^H + k_{-1'}^H)K_a^{NOH} \quad (11)$$

pH-jumps into methoxyacetic buffers led mainly to the formation of 2-(OMe,OTFE)H, especially at high buffer concentrations, while at low concentrations a mixture of all three products was observed (see below). Plots of k_{obsd} (Table S12)⁸ vs [CH₃OCH₂COOH] (not shown) were linear and gave pH-dependent slopes in the pH range from 3.94 to 5.36 (Table S13).⁸ Figure 4 shows a plot of (slope)^{−1} vs a_{H^+} according to eq 12

$$\frac{1}{\text{slope}} = \frac{1}{k_{-p}^{BH} + k_{-1}^{BH} + k_{-1'}^{BH}} + \frac{a_{H^+}}{K_a^{NOH}(k_{-p}^{BH} + k_{-1}^{BH} + k_{-1'}^{BH})} \quad (12)$$

which yields $k_{-p}^{BH} + k_{-1}^{BH} + k_{-1'}^{BH} = 0.36 \pm 0.03 \text{ M}^{-1} \text{ s}^{-1}$ and $pK_a^{NOH} = 4.81 \pm 0.05$. From eq 11 we now also obtain $k_{-p}^H + k_{-1}^H + k_{-1'}^H = 77.5 \pm 4.0 \text{ M}^{-1} \text{ s}^{-1}$.

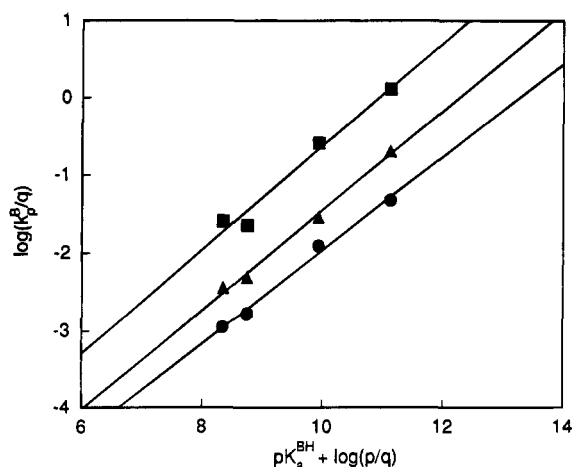
B. Product Ratios. In order to calculate individual rate constants in Scheme 2, product ratios had to be determined. These ratios were obtained by HPLC analysis as detailed in the Experimental Section. For pH-jumps into HCl solution we determined [1-OMe]:[1-OTFE]:[2-(OMe,OTFE)H] = 0.67:0.07:0.26 as the average from determinations at 220, 240, and 260 nm; the estimated error in these numbers is $\leq 5\%$. (For 2-(OMe,OTFE)H two HPLC peaks were observed in a ratio of 1.31 which we attributed to two different diastereomers.) In

Table 2. Brønsted β_B Values and Intrinsic Rate Constants for Proton Transfer in 50% Me₂SO–50% Water at 20 °C

	2-(OTFE) ₂ H	2-(OMe,OTFE)H	2-(OMe) ₂ H	PhCH ₂ NO ₂ ^d
$\beta(\text{RNH}_2)$	0.67 ± 0.08	0.64 ± 0.04	0.60 ± 0.04	
$\beta(\text{pip}/\text{mor})^b$	0.59	0.58	0.52	0.52
$\log k_0(\text{RNH}_2)$	-2.11 ± 0.08	-2.41 ± 0.05	-2.65 ± 0.06	
$\log k_0(\text{pip}/\text{mor})^b$	-1.86	-2.19	-2.42	-0.25
$\text{p}K_a^{\text{CH}}$	7.79 ± 0.07	8.51 ± 0.11	8.89 ± 0.06	8.23 ^c
$\text{p}K_a^{\text{NOH}}$	4.38 ± 0.08	4.81 ± 0.05	5.20 ± 0.10 ^d	4.75

^a Reference 7. ^b No standard deviations are available but estimated error is comparable to that for the parameters obtained with primary amines.

^c The actual $\text{p}K_a^{\text{CH}}$ is 7.93; the number in the table corrects for the fact that PhCH₂NO₂ has two equivalent protons while the various acetals have only one. ^d Reference 3.

**Figure 5.** Brønsted plots for the deprotonation of 2-(OTFE)₂H (squares), 2-(OMe,OTFE)H (triangles), and 2-(OMe)₂H (circles) by primary amines.

combination with $k_{-p}^H + k_{-1}^H + k_{-1'}^H = 77.5 \text{ M}^{-1} \text{ s}^{-1}$ determined above one now obtains $k_{-1}^H = 51.9 \text{ M}^{-1} \text{ s}^{-1}$, $k_{-1'}^H = 5.42 \text{ M}^{-1} \text{ s}^{-1}$, and $k_{-p}^H = 20.2 \text{ M}^{-1} \text{ s}^{-1}$; the estimated error in these rate constants is $\pm 10\%$.

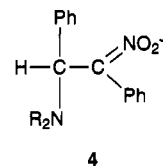
For the pH-jumps into methoxyacetic acid buffers, there is virtually no 1-OMe or 1-OTFE formed at $[\text{CH}_3\text{OCH}_2\text{COOH}] > 0.05 \text{ M}$, as indicated by UV spectra of the reaction solutions. This implies $k_{-p}^{\text{BH}} \gg k_{-1}^{\text{BH}} + k_{-1'}^{\text{BH}}$, and hence $k_{-p}^{\text{BH}} \approx k_{-p}^{\text{BH}} + k_{-1}^{\text{BH}} + k_{-1'}^{\text{BH}} = 0.36 \pm 0.03 \text{ M}^{-1} \text{ s}^{-1}$.

Discussion

Rates of Proton Transfer and $\text{p}K_a$ Values. Rate constants for the proton transfers according to eq 2 are summarized in Table 1. Brønsted plots for the deprotonation of 2-(OTFE)₂H, 2-(OMe,OTFE)H, and 2-(OMe)₂H by primary amines are shown in Figure 5; β_B values ($d(\log k_p^B)/d\text{p}K_a^{\text{BH}}$) and $\log k_0$ values, with k_0 being the intrinsic rate constant defined as $k_0 = k_1/q$ for $\text{p}K_a^{\text{BH}} - \text{p}K_a^{\text{CH}} + \log(p/q) = 0$ and obtained from the Brønsted plots, are reported in Table 2. Table 2 also includes β_B and $\log k_0$ values for the piperidine/morpholine pair, $\text{p}K_a^{\text{CH}}$ and $\text{p}K_a^{\text{NOH}}$ values, as well as corresponding parameters for phenylnitromethane.

The decrease in $\text{p}K_a^{\text{CH}}$ as well as in $\text{p}K_a^{\text{NOH}}$ resulting from substituting methoxy for trifluoroethoxy groups reflects the larger electron withdrawing inductive effect of the trifluoroethoxy group(s). Substituting one hydrogen of PhCH₂NO₂ by a PhC(OR,OR') moiety has a relatively small effect on $\text{p}K_a^{\text{CH}}$. This is most likely the result of two compensating factors. One is the electron withdrawing inductive effect of the PhC(OR,OR') moiety, the other the steric effect of the same moiety which prevents the nitronate ion from reaching perfect planarity and hence reduces its resonance stabilization. A similar steric

reduction in the resonance effect has been observed in amine adducts of α -nitrostilbenes (4)⁹ and even in PhC(CH₃)NO₂⁻.¹⁰



The dependence of the proton transfer rate constants on the $\text{p}K_a^{\text{BH}}$ of the bases leads to Brønsted β_B values that are consistent with similar values in the deprotonation of phenylnitromethane and other nitroalkanes. In view of the error limits associated with the β_B values, no significance should be attached to the slight variation in β_B with the structure of the acetal. On the basis of Bordwell and Boyle's¹⁰ study of aryl nitromethanes and ethanes no dependence of β_B is expected.

As to the intrinsic rate constants, the $\log k_0(\text{pip}/\text{mor})$ values are substantially lower for the three acetals than for the reaction of PhCH₂NO₂. This reduction must be mainly due to the large steric bulk of the acetals which hinders the approach of the relatively bulky secondary alicyclic amines. Another indication of the importance of the steric effect is the fact that the $\log k_0(\text{pip}/\text{mor})$ values are only about 0.25 log unit higher than the respective $\log k_0(\text{RNH}_2)$ for primary amines. In sterically unencumbered proton transfers from carbon, this difference is typically one log unit,^{7,11,12} reflecting the higher kinetic reactivity of alicyclic secondary compared to primary aliphatic amines.^{13,14} When there is significant steric hindrance in the transition state, the rate of the reaction with the bulkier alicyclic secondary amines is reduced more strongly than that with primary amines, which reduces the difference between $\log k_0(\text{pip}/\text{mor})$ and $\log k_0(\text{RNH}_2)$.

The dependence of the proton transfer rate constants on the $\text{p}K_a^{\text{CH}}$ of the acetal is of particular interest. Relevant Brønsted plots of $\log k_p^B$ vs $\log K_a^{\text{CH}}$ are shown in Figure 6. The slopes of these plots, α_{CH} (Table 3), are all greater than unity, indicating that k_p^B increases more strongly than K_a^{CH} . For the reverse rate constant, k_{-p}^{BH} , the corresponding Brønsted plots (not shown) have negative slopes ($\beta_C = 1 - \alpha_{\text{CH}}$), reflecting the fact that protonation of the nitronate ion becomes slower rather than faster with increasing basicity. These unusual Brønsted coefficients are reminiscent of the deprotonation of ArCH₂NO₂ and ArCH(CH₃)NO₂;¹⁰ they are a consequence of a highly imbalanced

(9) Bernasconi, C. F.; Renfrow, R. A. *J. Org. Chem.* **1987**, *52*, 3035.

(10) Bordwell, F. G.; Boyle, W. J., Jr. *J. Am. Chem. Soc.* **1972**, *94*, 3907.

(11) For a review, see: Bernasconi, C. F. *Adv. Phys. Org. Chem.* **1992**, *27*, 119.

(12) (a) Bernasconi, C. F.; Hibdon, S. A. *J. Am. Chem. Soc.* **1983**, *105*, 4343. (b) Bernasconi, C. F.; Bunnell, R. D. *Isr. J. Chem.* **1985**, *26*, 420.

(c) Bernasconi, C. F.; Paschalis, P. *J. Am. Chem. Soc.* **1986**, *108*, 2969. (d) Bernasconi, C. F.; Terrier, F. *Ibid.* **1987**, *109*, 7115.

(13) Jencks, W. P. *Catalysis in Chemistry and Enzymology*; McGraw-Hill: New York, 1969; p 178.

(14) Bell, R. P. *The Proton in Chemistry*, 2nd ed.; Cornell University Press: Ithaca, NY, 1973; Chapter 10.

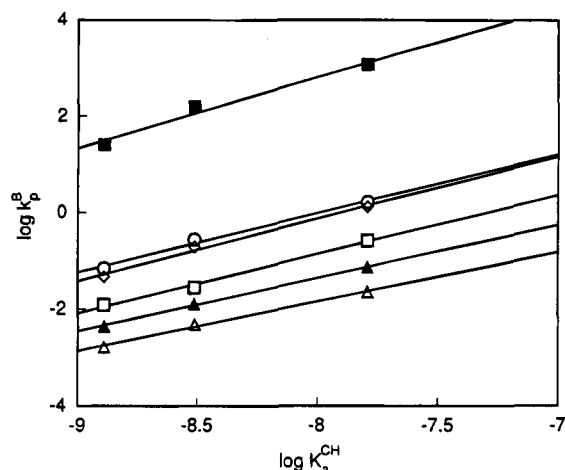


Figure 6. Brønsted plots for the deprotonation of **2-(OTFE)₂H**, **2-(OMe,OTFE)H**, and **2-(OMe)₂H** by OH[−] (■), piperidine (○), *n*-BuNH₂ (◇), CH₃OCH₂CH₂NH₂ (□), morpholine (▲), and H₂NCOCH₂NH₂ (Δ). The plot for EtOOCCH₂NH₂ is not shown to avoid clutter.

Table 3. Brønsted α_{CH} Values for Proton Transfer in 50% Me₂SO–50% Water at 20 °C

base	pK _a ^{BH}	α _{CH} (all) ^a	α _{CH} (two) ^b
OH [−]	17.34	1.47 ± 0.22	1.51
H ₂ O	−1.44		1.27 ^c
piperidine	11.02	1.22 ± 0.13	1.24
morpholine	8.72	1.09 ± 0.04	1.09
<i>n</i> -BuNH ₂	10.65	1.29 ± 0.14	1.31
CH ₃ OCH ₂ CH ₂ NH ₂	9.46	1.22 ± 0.09	1.20
H ₂ NCOCH ₂ NH ₂	8.27	1.22 ± 0.08	1.03
EtOOCCH ₂ NH ₂	7.87	1.01 ± 0.08	1.22
CH ₃ OCH ₂ COOH	4.56		1.50 ^c

^a Based on all three acetals; error limits are standard deviations.

^b Based on **2-(OTFE)₂H** and **2-(OMe)₂H** only; no standard deviations are available; experimental error may be assumed to be similar to the standard deviations in column "α_{CH}(all)." ^c Based on **2-(OTFE)₂H** and **2-(OMe,OTFE)H** only.

transition state in which the negative charge is mainly localized on the α-carbon, while in the nitronate ion it is mostly delocalized into the nitro group. Another manifestation of this imbalance is that inductively electron withdrawing substituents enhance the *intrinsic* rate constant,¹¹ as seen in the increase of log *k*₀(RNH₂) and log *k*₀(pip/mor) in the series **2-(OMe)₂H** → **2-(OMe,OTFE)H** → **2-(OTFE)₂H** (Table 2).

It should be noted that, as is the case for the dependence of β_B on the acetal pK_a^{CH}, the slight dependence of α_{CH} on pK_a^{BH} within a family of bases cannot be regarded as significant, owing to the sizable uncertainty in the α_{CH} values. As the cross relationship of eq 13¹⁵ requires, the absence of a pK_a^{CH} de-

$$p_{xy} = \partial \beta_B / \partial pK_a^{CH} = \partial \alpha_{CH} / -\partial pK_a^{BH} \quad (13)$$

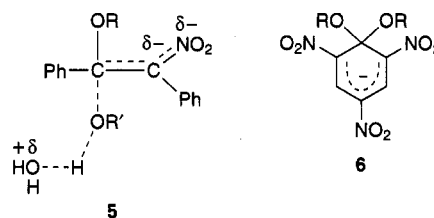
pendence of β_B is directly related to the lack of dependence of α_{CH} on pK_a^{BH}.

Competition between Protonation and Leaving Group Departure. Table 4 summarizes rate constants for protonation of the three adducts by H₃O⁺ and MeOCH₂COOH and of leaving group departure from the same adducts. The following features are noteworthy.

(1) As discussed in more detail elsewhere,⁴ the noncatalyzed loss of RO[−] depends strongly on the basicity of RO[−], as is apparent by comparing *k*_{−1} = 5.0 × 10^{−5} s^{−1} for CF₃CH₂O[−] loss (pK_a^{CH₃CH₂OH} = 14.0) from **2-(OMe,OTFE)[−]** with *k*_{−1}' = 4.0 × 10^{−8} s^{−1} for CH₃O[−] loss (pK_a^{CH₃OH} = 17.2) from

2-(OMe)₂[−] and *k*_{−1}' < (<<) 4.0 × 10^{−8} s^{−1} for CH₃O[−] loss from **2-(OMe,OTFE)[−]**. This strong dependence translates into a β_{lg} close to −1, implying a transition state in which C–O bond cleavage is far advanced. A comparison of *k*_{−1} = 5.0 × 10^{−5} s^{−1} for CF₃CH₂O[−] loss from **2-(OMe,OTFE)[−]** with the statistically corrected *k*_{−1}/2 = 0.82 × 10^{−5} for CF₃CH₂O[−] loss from **2-(OTFE)₂[−]** shows the importance of the combined influence of the stronger "push" by the methoxy group (increases *k*_{−1} for **2-(OMe,OTFE)[−]** compared to **2-(OTFE)₂[−]**) and the stronger inductive effect of the trifluoroethoxy group (lowers the *k*_{−1} for **2-(OTFE)₂[−]** compared to **2-(OMe,OTFE)[−]**). In fact the 6.1-fold acceleration of CF₃CH₂O[−] expulsion underestimates the magnitude of the combined influence of push and inductive effect because *k*_{−1} for **2-(OTFE)₂[−]** is enhanced by a steric effect,⁴ a point to which we will return below.

(2) In the H⁺ catalyzed loss of RO[−], the dependence on leaving group basicity is dramatically reduced and actually reversed, as is apparent from the comparison of *k*₁^H = 51.9 M^{−1} s^{−1} for CF₃CH₂O[−] loss from **2-(OMe,OTFE)[−]** with *k*₁^H = 7.46 × 10² M^{−1} s^{−1} for CH₃O[−] loss from **2(OMe)₂[−]**; even after statistical correction of the latter (3.73 × 10² M^{−1} s^{−1}), CH₃O[−] loss is still seen to be considerably faster than CF₃CH₂O[−] loss. Apparently, the high basicity of the methoxy leaving group renders its protonation in the transition state (**5**) so much more favorable than the protonation of the trifluoro-



ethoxy group that this more than offsets the inherent weaker nucleofugality of the methoxy leaving group. A similar reversal in relative nucleofugalities has been observed in 1,1-dialkoxy Meisenheimer complexes (**6**) with R = CH₃CH₂, CH₃, CH₃OCH₂CH₂, ClCH₂CH₂, and HC≡CCH₂.¹⁶

(3) The combined effect of the stronger push and weaker inductive effect of the methoxy relative to the trifluoroethoxy group is even more apparent in the acid catalyzed compared to the noncatalyzed reactions. This is seen from the statistically corrected *k*₁^H/2 = 3.73 × 10² M^{−1} s^{−1} for CH₃O[−] expulsion from **2-(OMe)₂[−]** which is 69-fold larger than *k*₁^H' = 5.42 M^{−1} s^{−1} for CH₃O[−] expulsion from **2-(OMe,OTFE)[−]**, or from *k*₁^H = 51.9 M^{−1} s^{−1} for CF₃CH₂O[−] expulsion from **2-(OMe,OTFE)[−]** which is 125-fold higher than the statistically corrected *k*₁^H/2 = 0.41 M^{−1} s^{−1} for CF₃CH₂O[−] expulsion from **2-(OTFE)₂[−]**. The seemingly stronger influence of push/inductive effect in the acid catalyzed reaction may be a consequence of a reduced steric effect; as discussed above, the stronger crowding in **2-(OTFE)₂[−]** compared to **2-(OMe,OTFE)[−]**, and presumably in **2-(OMe,OTFE)[−]** compared to **2-(OMe)₂[−]**, counteracts the influence of the increased push/reduced inductive effect by the methoxy group. A possible reason why the steric effect is reduced in the acid catalyzed reaction is that the transition state is more adduct-like than in the uncatalyzed reaction, as predicted by the Hammond¹⁷–Leffler¹⁸ postulate. This interpretation is not without problems, though.¹⁹

(4) The reaction why the reaction of **2-(OTFE)₂[−]** with acid leads virtually exclusively to the acetal by protonation, whereas the reaction of **2-(OMe)₂[−]** leads virtually exclusively to **1-OMe** by CH₃O[−] expulsion, is the result of two factors. The first is

(15) (a) Jencks, D. A.; Jencks, W. P. *J. Am. Chem. Soc.* **1977**, *99*, 7948. (b) Jencks, W. P. *Chem. Rev.* **1985**, *85*, 511.

(16) Bernasconi, C. F.; Gandler, J. R. *J. Am. Chem. Soc.* **1978**, *100*, 8117.

Table 4. Rate Constants of the Reactions of Various Intermediates in the Presence and Absence of Acid in 50% Me₂SO–50% Water at 20 °C^a

	2-(OTFE) ₂ [−]	2-(OMe, OTFE) [−]	2-(OMe) ₂ [−] ^e
	Loss of RO [−]		
k_{-1} , s ^{−1}	1.65 × 10 ^{−5} (OTFE) ^{b,d}	5.0 × 10 ^{−5} (OTFE) ^b	
$k_{-1'}$, s ^{−1}		<(≪)4 × 10 ^{−8} (OMe) ^c	4.0 × 10 ^{−8} (OMe) ^{c,d}
k_{-1}^H , M ^{−1} s ^{−1}	0.80 (OTFE) ^{a,c}	51.9 (OTFE) ^b	
$k_{-1'}^H$, M ^{−1} s ^{−1}		5.42 (OMe) ^c	7.46 × 10 ² (OMe) ^{c,d}
	Protonation		
k_{-p}^H , M ^{−1} s ^{−1}	31.4	20.2	≈16 ^f
$k_{-p}^{MeOAcOH}$, M ^{−1} s ^{−1}	8.16 × 10 ^{−1}	3.60 × 10 ^{−1}	

^a Rate constants defined according to Scheme 2. ^b CF₃CH₂O[−] departure. ^c CH₃O[−] departure. ^d Not statistically corrected. ^e References 3 and 4.^f Estimated based on k_{-p}^H for 2-(OTFE)₂[−] and 2-(OMe, OTFE)[−] and $\beta_C = 1 - \alpha_{CH} \approx -0.27$.

the combination of stronger H⁺ catalysis in the departure of the more basic CH₃O[−] and the stronger push/weaker inductive effect by the methoxy group which makes H⁺ catalyzed CH₃O[−] expulsion from 2-(OMe)₂[−] almost 10³-fold faster than H⁺ catalyzed CF₃CH₂O[−] departure from 2-(OTFE)₂[−]. The second is that the enhanced pK_a^{CH} of 2-(OMe)₂[−] compared to 2-(OTFE)₂[−] does not lead to an enhanced rate of protonation (k_{-p}^H) which could partially offset the increase in k_{-1}^H . On the contrary, k_{-p}^H is somewhat lower for 2-(OMe)₂[−] than for 2-(OTFE)₂[−], a consequence of the anomalous behavior of nitroalkanes discussed above.

Experimental Section

Materials. 1,1-Dimethoxy-1,2-diphenyl-2-nitroethane, 2-(OMe)₂H, was obtained as a minor byproduct in the synthesis of 1-OMe by reaction of 1-I with NaOMe as follows. A solution containing 0.5 g (1.4 mmol) of 1-I and 116 mg (2.15 mmol) of NaOMe in a mixture of 1.5 mL of MeOH and 25 mL of MeCN was stirred in the dark at room temperature for 1 week. This reaction mixture was then poured into 50 mL of an aqueous 1 N HCl solution and extracted with CHCl₃ (2 × 30 mL). The organic phase was separated, washed with 5% Na₂S₂O₃ solution (30 mL) and then with water (2 × 25 mL), dried (MgSO₄), and evaporated. The yellow oil obtained (360 mg) was chromatographed on a silica column using 1:1 CH₂Cl₂–petroleum ether (40–60 °C) as eluent. Three fractions were identified: diphenylacetylene (19 mg, 8%), mp 58 °C, 1-OMe (91 mg, 25%), mp 82 °C, and 1,1-dimethoxy-1,2-diphenyl-2-nitroethane, 2-(OMe)₂H (10 mg, 2.5%). Fifty five milligrams (11%) of the starting material, 1-I, were also recovered; furthermore, TLC showed six other compounds that were not identified or analyzed. Crystallization of 2-(OMe)₂H from 1:1 hexane–cyclohexane gave needles, mp 110 °C. ¹H NMR (CDCl₃) δ 3.18, 3.52 (6H, 2s, 2 prochiral CH₃O), 6.13 (1H, s, CH), 7.03–7.34 (10H, m, Ph). MS, 70 eV, 90 °C (m/z , relative abundance, assignment): 241 (5%, M – NO₂), 210 (32%, M – NO₂ – MeO), 178 (6%, PhC≡CPh), 167 (40%), 165 (40%), 152 (66%, PhCH(OMe)₂), 151 (100%, PhC(OMe)₂), 91 (60%, C₇H₇). Anal. Calcd for C₁₆H₁₇NO₄: C, 66.89; H, 5.96; N, 4.88. Found: C, 66.79; H, 5.27; N, 4.70%.

1,1-Di(2,2,2-trifluoroethoxy)-1,2-diphenyl-2-nitroethane, 2-(OTFE)₂H, was available from a previous study.⁴ 1-Methoxy-1-(2,2,2-trifluoroethoxy)-1,2-diphenyl-2-nitroethane, 2-(OMe,OTFE)H, was generated in situ by reaction of 2-(OMe,OTFE)[−] with a methoxyacetate buffer at pH 4.56; 2-(OMe,OTFE)[−], in turn, was generated by adding 1-OMe to a CF₃CH₂O[−] buffer as described previously.⁴

Trifluoroethanol was distilled prior to use. The amines were dried and freshly distilled over CaH₂ before use. DMSO was stiller over CaH₂ under vacuum. Methoxyacetic acid (Aldrich) was used without further purification. HCl and KOH solutions were prepared from "Dilut-it" (Baker) by appropriate dilution with filtered deionized water.

(17) Hammond, G. S. *J. Am. Chem. Soc.* **1955**, 77, 334.(18) Lefler, J. E.; Grunwald, E. *Rates and Equilibria of Organic Reactions*; Wiley, New York, 1963; p 156.

(19) One problem is that a more adduct-like transition state implies not only a weaker steric effect but also a reduced push/inductive effect. Hence the larger rate factor in the acid catalyzed reaction requires that the more adduct-like transition state leads to a stronger attenuation of the steric effect than of the push/inductive effect.

HPLC-grade acetonitrile (Alltech) was filtered and degassed with He before use in HPLC experiments.

Reaction Solutions and pH Determinations. The procedures were the same as described previously.⁴

Kinetic Measurements. Most proton transfer rates were determined in the direction 2-(OR,OR')H → 2-(OR,OR')[−]. Determinations via pH-jump experiments in the 2-(OR,OR')[−] → 2-(OR,OR')H direction were made for the reactions of 2-(OTFE)₂[−] and 2-(OMe,OTFE)[−] with HCl and MeOCH₂COOH and of 2-(OMe)₂[−] with EtOOCCH₂NH₃⁺.

The rates of the reactions with OH[−] and CF₃CH₂O[−] were measured in an Applied Photophysics DX.17MV stopped-flow apparatus, the others in a Perkin-Elmer Lambda 2 spectrophotometer. The reactions were monitored around 272 nm which is at or near λ_{max} of the 2-(OR,OR')[−] adducts. The kinetic traces were fitted by means of the nonlinear regression program, Enzfitter.²⁰

Product Study of the Reactions of 2-(OMe,OTFE)[−] and 2-(OTFE)₂[−] with Acid. The product analysis was conducted in a 1090M Hewlett-Packard HPLC instrument using a C₁₈ reverse phase column and a flow rate of 1.5 mL/min. Mobile phase: solvent A, 30% CH₃CN–70% H₂O; solvent B, 80% CH₃CN–20% H₂O; 100% A for 2 min, 0 to 100% B for 20 min, 100% B for 8 min.

The reaction samples were diluted 10-fold with water prior to injection into the HPLC column; this reduction of the DMSO content to 5% improved the separation. The retention times were 19.6 and 21.2 min for 1-OMe and 1-OTFE, respectively; for the two diastereomers of 2-(OMe,OTFE)H the retention times were 22.7 and 22.9 min. Yields of the products were calculated from the HPLC areas using Beers' calibration plots of 1-OMe for both 1-OMe and 1-OTFE and of 2-(OTFE)₂H for 1-(OMe,OTFE)H. This procedure is based on the assumption that the extinction coefficients of 1-OTFE at the three analytical wavelengths used (220, 240, and 260 nm) are the same as for 1-OMe, and those of 2-(OMe,OTFE)H are the same as for 2-(OTFE)₂H. Since the UV spectra taken by the diode array spectrophotometer of the HPLC instrument showed that the spectrum of 1-OTFE is virtually identical to that of 1-OMe, and that of 2-(OMe,OTFE)H is virtually identical to that of 2-(OTFE)₂H, these assumptions are justified.

Acknowledgment. This research was supported by Grants Nos. CHE-8921739 and CHE-9307659 from the National Science Foundation (C.F.B.) and a grant from the U.S.–Israel Binational Science Foundation, Jerusalem, Israel (Z.R.). Acknowledgment is also made to the donors of the Petroleum Research Fund, administered by the American Chemical Society, for partial support of this research (grant 26506-AC4 to C.F.B.).

Supplementary Material Available: Tables S1–S15, kinetic data for reactions of 2-(OTFE)₂H, 2-(OTFE)₂[−], 2-(OMe)₂H, 2-(OMe,OTFE)H, and 2-(OMe,OTFE)[−] (17 pages). This material is contained in many libraries on microfiche, immediately follows this article in the microfilm version of the journal, can be ordered from the ACS, and can be downloaded from the Internet; see any current masthead page for ordering information and Internet access instructions.

JA943221B

(20) Program written by R. J. Leatherbarrow.